

Cold Collision Frequency Shift of the 1S-2S Transition in Hydrogen

Thomas C. Killian, Dale G. Fried, Lorenz Willmann, David Landhuis, Stephen C. Moss,
Thomas J. Greytak, and Daniel Kleppner

*Department of Physics and Center for Materials Science and Engineering,
Massachusetts Institute of Technology, Cambridge, Massachusetts 02139*

(Accepted for publication in Physical Review Letters: October 2, 1998)

Abstract

We have observed the cold collision frequency shift of the 1S-2S transition in trapped spin-polarized atomic hydrogen. We find $\Delta\nu_{1S-2S} = -3.8 \pm 0.8 \times 10^{-10} n \text{ Hz cm}^3$, where n is the sample density. From this we derive the 1S-2S s -wave triplet scattering length, $a_{1S-2S} = -1.4 \pm 0.3 \text{ nm}$, which is in fair agreement with a recent calculation. The shift provides a valuable probe of the distribution of densities in a trapped sample.

Methods for cooling and trapping neutral atoms have opened a low energy regime where collisional phenomena involve only a single partial wave. The ground state s -wave scattering lengths for many of the alkali metal atoms have been obtained from combinations of theory and experiment. Those studies were motivated in part by the need to estimate evaporative cooling rates [1], study the stability of Bose-Einstein condensates [2,3], and understand collisional shifts of atomic fountain frequency standards [4,5].

We have measured a density-dependent frequency shift of the two-photon $1S$ - $2S$ transition in trapped atomic hydrogen. This allows us to deduce the $1S$ - $2S$ triplet scattering length, which has been calculated by Jamieson, Dalgarno, and Doyle [6]. The frequency shift also provides a probe of the density distribution of our trapped sample, and constitutes a valuable tool for the study of Bose-Einstein condensation. (See the accompanying paper on BEC in atomic hydrogen [7].)

Interactions between neighboring atoms shift and broaden atomic spectral lines. For bosons at low temperatures, where only s -wave collisions occur (below about 1 K for H [8]), the elastic contribution to the shift can be described through the density-dependent mean field level shift [9]

$$E = \frac{8\pi\hbar^2 an}{m}. \quad (1)$$

Here, a is the atom's s -wave scattering length for collisions in the gas, and all particles have mass m . The gas has density n , and is assumed to be nondegenerate. The difference between the mean field energy in the excited and ground states results in a frequency shift. For weak excitation of the $1S$ - $2S$ transition in spin-polarized hydrogen,

$$\Delta\nu_{1S-2S} = (a_{1S-2S} - a_{1S-1S}) \frac{4\hbar n_{1S}}{m}, \quad (2)$$

where the scattering lengths are for the triplet potentials.

Additional contributions to the shift can result from inelastic processes. The most important corrections should arise from collisional hyperfine transitions and quenching of the $2S$ state. Hyperfine transitions in the spin-polarized sample arise only through weak magnetic dipole interactions [10], and in our experiment we observe no evidence for collisional quenching on a millisecond time scale. Thus it is reasonable to neglect inelastic processes when describing the observed density-dependent frequency shift.

Analogous frequency shifts are observed in hydrogen masers [11] and cesium atomic fountains [12]. Using the collision-based formalism commonly applied to these systems, one can derive Eq. 2 and also show that homogeneous broadening due to elastic collisions is negligible in the present study because the phase shift per collision, $2\pi a/\lambda_{\text{deBroglie}}$, is small.

Our techniques for cooling and trapping hydrogen have been described elsewhere [13] and are only briefly summarized here. Molecules are dissociated in a cryogenic discharge, and the atoms thermalize by collisions with the 250 mK liquid ^4He -coated cell wall and each other. A fraction of the “low-field seeking” $F = 1, m_F = 1$ atoms settle into the magnetic field minimum of a 500 mK deep Ioffe-Pritchard magnetic trap [14] (Fig. 1). An axial bias field of a few gauss in the trapping region inhibits nonadiabatic spin flips.

The wall temperature is decreased to 120 mK. This increases the wall residence time of H atoms, facilitating recombination, so that contact with the wall effectively removes energetic

atoms. This process initiates evaporative cooling [15,16] and thermally disconnects the sample from the wall. The evaporation is forced by decreasing the trap depth, which is set by a saddlepoint in the magnetic field. Sample temperatures as low as 110 μK and densities approaching 10^{14} cm^{-3} are achieved. Under these conditions the sample is a needle-shaped cloud with a diameter of 200 μm and a length of 8 cm.

The speed with which the trap threshold can be lowered is limited by the need to maintain thermal equilibrium through elastic collisions during the evaporation. After the forced evaporation is terminated, the sample temperature remains constant. Its value is determined by the balance between cooling due to evaporation of atoms over the threshold and heating due to dipolar spin-flip collisions. Dipolar decay preferentially removes atoms from the bottom of the trap where the density is highest.

The temperature [17] and density [16] are measured by rapidly lowering the trap threshold to zero while monitoring the power deposited on a bolometer. The power results from molecular recombination and is proportional to the flux of atoms escaping from the trap. The dependence of the flux on the threshold reveals the energy distribution of atoms in the trap, which, combined with a knowledge of the trapping fields, yields the sample temperature.

We measure the density by releasing the atoms from the trap after holding them for different times t following the forced evaporation. The total recombination energy deposited on the bolometer is proportional to $N(t)$, the number of atoms remaining in the trap at time t . $N(t)$ decreases with time due to dipolar decay, which removes atoms from the sample at a density-dependent rate (Fig. 2). This process obeys the two-body equation $dn/dt = -gn^2$, where n is the local density and $g = 1.1 \times 10^{-15} \text{ cm}^3/\text{s}$ is the calculated rate constant [10,18]. When averaged over the density distribution in the trap, this implies that $N(t)$ obeys [16]

$$N(0)/N(t) = 1 + \kappa gn_0(0)t. \quad (3)$$

Here, $n_0(t)$ is the maximum density in the sample at time t , and κ is a numerical factor which depends on the trap geometry. Computations show that κ is typically in the range 0.2–0.3. For a given geometry, the uncertainty in κ is 10%, arising from imperfect knowledge of the magnetic fields. The number of atoms for a given trapping configuration is reproducible to a few percent.

Once the sample temperature and density are known, we measure the cold collision frequency shift by two-photon Doppler-free $1S$ - $2S$ spectroscopy [19]. The 243 nm laser that excites atoms to the metastable $2S$ state is stabilized by an optical cavity and has a linewidth of about 1 kHz. 8 mW of radiation is focused to a waist radius of $w_0 = 50 \mu\text{m}$ in the trap. The beam lies along the axis of the atom cloud and is retro-reflected by a spherical mirror to provide the standing wave required for Doppler-free excitation. A mechanical chopper pulses the laser beam at 1 kHz with a 50% duty cycle. Following each pulse, an electric field of 10 V/cm Stark-quenches the excited atoms by mixing the $2S$ and $2P$ wavefunctions. This causes prompt radiative decay by emission of a Lyman- α photon (122 nm). The emitted photons are counted using a microchannel plate detector located at the end of the trap, behind the retro-reflecting mirror. Due to the low collection solid angle (2×10^{-2} ster), absorptive losses, and detector quantum efficiency, the total detection efficiency is only 10^{-5} .

Typical data for determining the cold collision frequency shift is shown in Fig. 3a. The density is highest immediately after the forced evaporation, so the first recorded spectrum

is shifted the most. Due to the distribution of densities in the sample, the line is inhomogeneously broadened. The density decreases on a 20 s time scale primarily due to collisions with helium atoms evaporated from the mirror surface by the laser; hence successive scans probe different densities. The later spectra exhibit the exponential lineshape, $\exp(-|\nu|/\delta\nu_{\text{transit}})$ [20], expected for Doppler-free two-photon excitation by a Gaussian laser beam of a low density sample. Here, ν is the laser detuning from resonance at 243 nm in Hz, $\delta\nu_{\text{transit}} = \sqrt{2k_B T/m}/(4\pi w_0)$ is the linewidth due to the finite interaction time of an atom with the laser beam – typically 2–5 kHz. Measurement of the low density linewidth provides an independent check of our sample temperature [19].

To quantify the cold collision frequency shift, one must account for the distribution of densities in the trap. Numerical simulations of the spectra show that the shift of the line center is about 0.75 of the shift associated with the maximum density in the sample, n_0 . This factor depends on the trapping magnetic fields, sample temperature, and laser focus position with respect to the atom cloud. There is a 10% uncertainty in this correction for a given configuration.

The integral of the $1S$ - $2S$ spectrum is proportional to $n_0(t)$, and it decreases smoothly in time. This allows us to extrapolate from the initial density before the first scan, found as described above, to determine the density for each successive scan. A fit to data such as shown in Fig. 3b yields χ , where $\chi = \Delta\nu_{1S-2S}/n$. Measurement errors are small compared to the mentioned systematic uncertainties. The long term drift of the laser frequency, ~ 10 kHz/hour, is taken into account. Note that no knowledge of absolute frequency is required to determine χ from a given series of scans.

To examine the sensitivity to systematic effects, χ was measured in different trap configurations, with sample temperatures between 110 and 500 μK and initial maximum densities in the range $(2 \sim 7) \times 10^{13} \text{ cm}^{-3}$. In Fig. 4, the various measurements are plotted versus sample temperature. We observe no significant temperature dependence of the shift, consistent with theory. Any significant nonlinear density dependence of the shift would manifest itself in data such as Fig. 3b, but none is evident.

From a weighted average of the various measurements, we find $\chi = -3.8 \pm 0.8 \times 10^{-10} \text{ Hz cm}^3$. In an apparatus optimized for spectroscopy with better known magnetic field and laser geometries, the uncertainty could be greatly reduced. A revision of the calculated value for g would cause a proportional change in the value of χ . Experiments have verified this decay constant at the 20% level [21], but since the calculation involves well known ground state potentials, the calculated value is expected to be more certain.

Equation 2 relates χ to the s -wave triplet scattering lengths, assuming inelastic processes can be neglected. From this, we derive $a_{1S-2S} = -1.4 \pm 0.3 \text{ nm}$. We have used the theoretical value of $a_{1S-1S} = 0.0648 \text{ nm}$ [22], which constitutes only a small contribution to χ . The value calculated by Jamieson *et al.* [6], $a_{1S-2S} = -2.3 \text{ nm}$, is in fair agreement with this measurement.

Having calibrated the cold collision frequency shift, we can use two-photon spectroscopy to measure sample density provided the shift is comparable to or greater than the transit-time width, $\delta\nu_{\text{transit}}$. The spectrum, $S(\nu)$, is given by the approximate expression

$$S(\nu) \propto \int d^3\mathbf{r} n(\mathbf{r}) I^2(\mathbf{r}) \delta(\nu - \chi n(\mathbf{r})), \quad (4)$$

which neglects atomic motion and laser linewidth. $I(\mathbf{r})$ is the laser intensity, and the delta

function enforces the resonance condition. In our experiment, at high densities and low temperatures, and especially in the regime of Bose-Einstein condensation, this probe is more sensitive and accurate than the bolometer. In addition, it provides valuable information on the density distribution [7].

$1S$ - $2S$ spectroscopy of cold trapped hydrogen can be used for optical frequency metrology and precision measurements. Linewidths of about 1 kHz have been achieved in an atomic beam [23], but with the long coherence time possible in a trap [19] it should be feasible to approach the 1.3 Hz natural linewidth of the transition. To reduce the effects of the cold collision shift below this level, it is desirable to work at densities of $\leq 10^{10}$ cm $^{-3}$. Even with such a decreased density, large signal rates are still possible in an apparatus optimized for optical access.

We thank Jon C. Sandberg and Claudio L. Cesar for construction of the laser system used in this experiment and development of two-photon spectroscopy of trapped hydrogen. We are also grateful to Alexander Dalgarno for helpful discussions.

This work is funded by the National Science Foundation and the Office of Naval Research. Early support came from the Air Force Office of Scientific Research. L.W. acknowledges support by Deutsche Forschungsgemeinschaft. D.L. and S.C.M. are supported by National Defense Science and Engineering Graduate Fellowships.

REFERENCES

- [1] W. Ketterle and N. J. van Druten, in *Advances in Atomic, Molecular, and Optical Physics*, edited by B. Bederson and H. Walther (Academic Press, San Diego, 1996), No. 37, p.181.
- [2] C. J. Myatt, E. A. Burt, R. W. Ghrist, E. A. Cornell, and C. E. Wieman, *Phys. Rev. Lett.* **78**, 586 (1997).
- [3] C. C. Bradley, C. A. Sackett, and R. G. Hulet, *Phys. Rev. Lett.* **78**, 985 (1997).
- [4] K. Gibble and S. Chu, *Phys. Rev. Lett.* **70**, 1771 (1993).
- [5] S. J. J. M. F. Kokkelmans, B. J. Verhaar, K. Gibble, and D. J. Heinzen, *Phys. Rev. A* **56**, R4389 (1997).
- [6] M. J. Jamieson, A. Dalgarno, and J. M. Doyle, *Mol. Phys.* **87**, 817 (1996).
- [7] D. G. Fried, T. C. Killian, L. Willmann, D. Landhuis, S. C. Moss, D. Kleppner, and T. J. Greytak, *Phys. Rev. Lett.* to be published, (1998).
- [8] P. S. Julienne and F. H. Mies, *J. Opt. Soc. Am. B* **6**, 2257 (1989).
- [9] R. K. Pathria, *Statistical Mechanics* (Pergamon Press, New York, 1972), p. 300; E. P. Bashkin, *Pis'ma Zh. Eksp. Teor. Fiz.* **33**, 11 (1981) [*JETP Lett.* **33** 8 (1981)].
- [10] H. T. C. Stoof, J. M. V. A. Koelman, and B. J. Verhaar, *Phys. Rev. B* **38**, 4688 (1988).
- [11] B. J. Verhaar, J. M. V. A. Koelman, H. T. C. Stoof, and O. J. Luiten, *Phys. Rev. A* **35**, 3825 (1987).
- [12] E. Tiesinga, B. J. Verhaar, H. T. C. Stoof, and D. van Bragt, *Phys. Rev. A* **45**, R2671 (1992).
- [13] T. J. Greytak, in *Bose-Einstein Condensation*, edited by A. Griffin, D. W. Snoke, and S. Stringari, (Cambridge University Press, 1995), p. 131.
- [14] D. Pritchard, *Phys. Rev. Lett.* **51**, 1336 (1983).
- [15] H. Hess, *Phys. Rev. B* **34**, 3476 (1986).
- [16] N. Masuhara, J. M. Doyle, J. C. Sandberg, D. Kleppner, T. J. Greytak, H. F. Hess, and G. P. Kochanski, *Phys. Rev. Lett.* **61**, 935 (1988).
- [17] J. M. Doyle, J. C. Sandberg, N. Masuhara, I. A. Yu, D. Kleppner, and T. J. Greytak, *J. Opt. Soc. Am. B* **6**, 2244 (1989).
- [18] We calculate the rate constant $g = 2(G_{dd \rightarrow ac} + G_{dd \rightarrow aa} + G_{dd \rightarrow ad})$, using zero temperature and zero field values of the decay event rates, G . Atoms ending in the c and d states after a spin flip are lost from the trap because the hyperfine energy (71 mK) is much greater than the trap depths used in this study.
- [19] C. L. Cesar, D. G. Fried, T. C. Killian, A. D. Polcyn, J. C. Sandberg, I. A. Yu, T. J. Greytak, D. Kleppner, and J. M. Doyle, *Phys. Rev. Lett.* **77**, 255 (1996).
- [20] C. Bordé, *C. R. Hebd. Séan. Acad. Sci. B* **282**, 341 (1976); F. Biraben, M. Bassini, and B. Cagnac, *J. Phys. (Paris)* **40**, 445 (1979).
- [21] R. van Roijen, J. J. Berkhout, S. Jaakola, and J. T. M. Walraven, *Phys. Rev. Lett.* **61**, 931 (1988).
- [22] M. J. Jamieson, A. Dalgarno, and M. Kimura, *Phys. Rev. A* **51**, 2626 (1995). This calculation uses an improved *ab initio* $1S-1S$ potential which changes the scattering length from previous values. See discussion in the cited paper.
- [23] T. Udem, A. Huber, B. Gross, J. Reichert, M. Prevedelli, M. Weitz, and T. W. Hänsch, *Phys. Rev. Lett.* **79**, 2646 (1997).

FIGURES

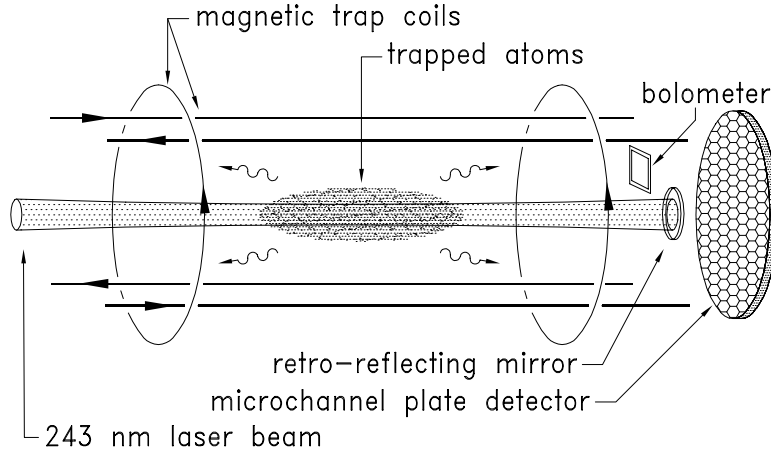


FIG. 1. Schematic diagram of the apparatus. Coils create a magnetic field with a minimum along the trap axis, which confines the sample. The 243 nm laser beam is focused to a $50 \mu\text{m}$ beam radius and retroreflected. A $500 \mu\text{s}$ laser pulse promotes some atoms to the metastable $2S$ state. An electric field then Stark-quenches the $2S$ atoms, and the resulting Lyman- α fluorescence photons are counted by the microchannel plate. Not shown is the trapping cell which surrounds the sample and is thermally anchored to a dilution refrigerator. The actual trap is longer and narrower than indicated in the diagram.

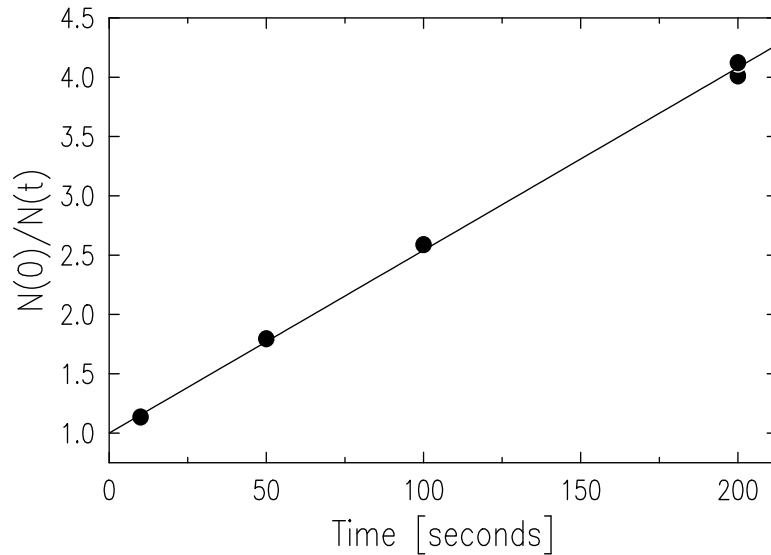


FIG. 2. Dipolar decay of trapped hydrogen. The sample density is found from the slope of $N(0)/N(t)$, the inverse of the normalized total number of atoms remaining in the trap. The data shown indicates a density of $6.0 \times 10^{13} \text{ cm}^{-3}$.

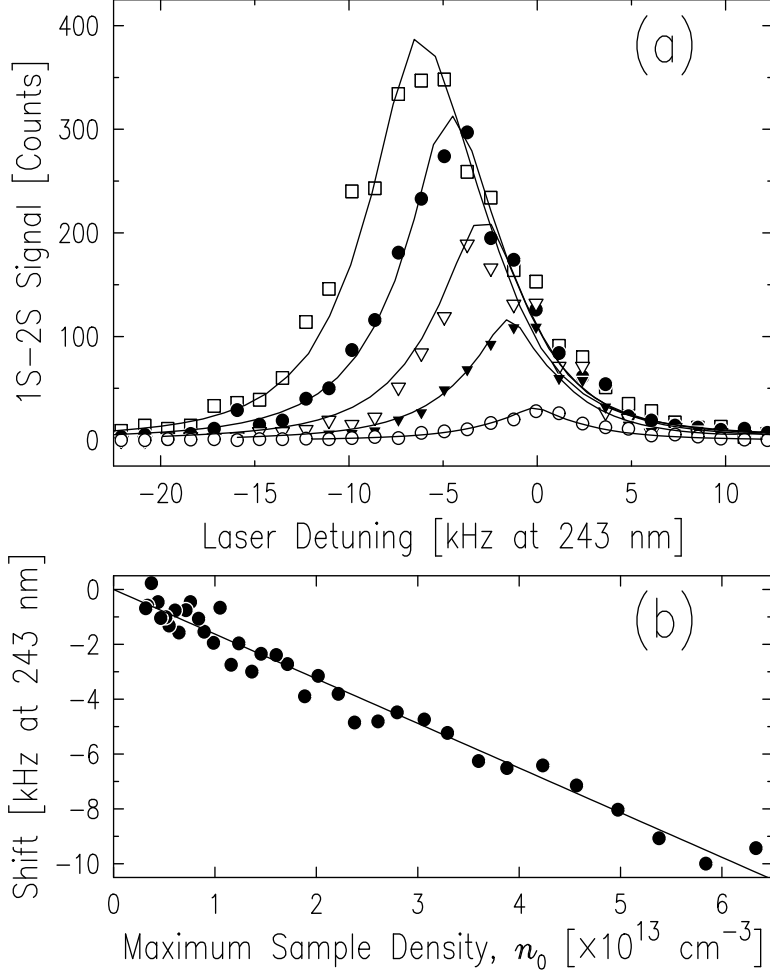


FIG. 3. (a) Cold collision frequency shift observed in the spectra of a single $120 \mu\text{K}$ sample with initial maximum density of $n_0(0) = 6.6 \times 10^{13} \text{ cm}^{-3}$. The furthest red-shifted spectrum was recorded first, and subsequent spectra were taken at decreasing sample densities. Each data point represents 12 ms of laser excitation and one scan is recorded in 0.5 seconds. 20 seconds elapsed between the first and last scan shown. The smooth curves are the result of numerical simulation. Only 5 of the 40 spectra taken of this sample are shown.

(b) Frequency shifts from spectra of sample described in (a) after correcting for inhomogeneous sample density. For this data, the linear fit yields $\chi = -3.30 \pm 0.6 \times 10^{-10} \text{ Hz cm}^3$, where $\chi = \Delta\nu_{1S-2S}/n$. (Note, $\Delta\nu_{1S-2S}$, the shift in the transition frequency, is twice the shift in the frequency of the 243 nm laser.)

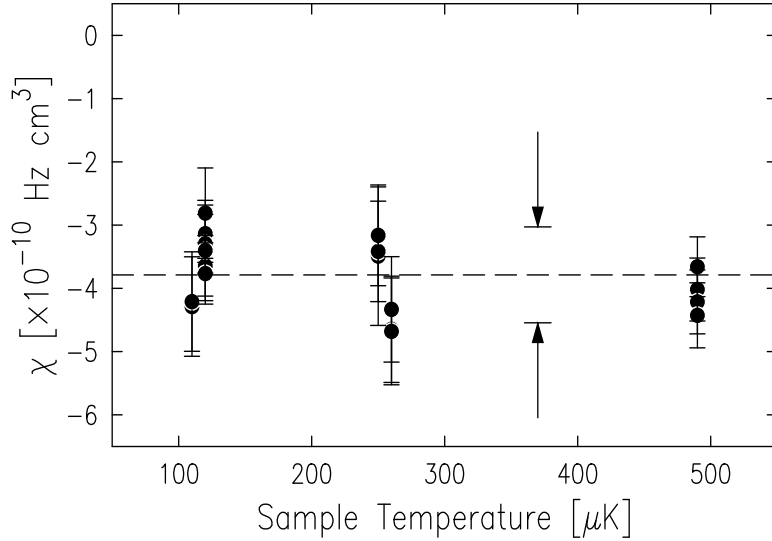


FIG. 4. The frequency shift parameter χ , determined as described in Fig. 3 for various trap configurations. No significant dependence on sample temperature is observed. The error bars reflect systematic uncertainties in the magnetic trapping fields and laser geometry, with small contributions from measurement error. The dashed line is the weighted mean of all measurements, $\chi = -3.8 \pm 0.8 \times 10^{-10}$ Hz cm^3 , and the quoted uncertainty is indicated by the double arrows.